Journal of Rehabilitation in Civil Engineering 10-3 (2022) 37-63

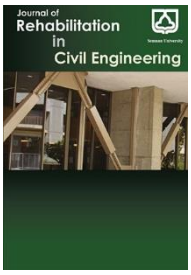

journal homepage: http://civiljournal.semnan.ac.ir/

Damage Detection in Prestressed Concrete Slabs Using Wavelet Analysis of Vibration Responses in the Time Domain

Hashem Jahangir[1], Mohsen Khatibinia[2*], Mehran Mokhtari Masinaei[3]

1. Assistant Professor, Department of Civil Engineering, University of Birjand, Birjand, Iran
2. Associate Professor, Department of Civil Engineering, University of Birjand, Birjand, Iran
3. M.Sc. in Structural Engineering, Civil Engineering Department, Hormozan University of Birjand, Birjand, Iran
Corresponding author: *m.khatibinia@birjand.ac.ir*

ARTICLE INFO

Article history:
Received: 09 May 2021
Revised: 08 September 2021
Accepted: 16 October 2021

Keywords:
Damage detection;
Vibration responses;
Time domain;
Wavelet transform;
Prestressed concrete slabs.

ABSTRACT

Detection of damages in structures during their service life is of vital importance and under attention of researchers. In this paper, it is attempted to identify damages in prestressed concrete slabs using vibration responses obtained from modal testing in the time domain. For this purpose, first some damage scenarios with various geometric shapes and at different locations of numerical models, corresponding to a prestressed concrete slab, were created. Next, the impact hammer force in the modal test was simulated and the accelerations time histories at different degrees of freedom corresponding to the numerical models per two states of damaged and undamaged structure were selected as the inputs for a number of damage indices to identify the damage locations. Some of these damage scenarios have been located at the middle of prestressed concrete slabs and some at the corners. The proposed damage indices in this research are obtained based on the area under the diagram of acceleration time histories, maximum and also the area under diagram of detail coefficients of the wavelet transform using the three wavelet families of Daubechies, Biorthogonal and Reverse Biorthogonal. The results showed that using damage index obtained from the area under diagram of detail coefficients of wavelet transform with the mother wavelet db2 could detect the damage scenarios at the middle and corners of the slab with a well precision. Furthermore, the damage scenarios at the corners of numerical models could be detected properly by using the mother wavelet rbio2.2 in the proposed damage index.

How to cite this article:
Jahangir, H., Khatibinia, M., Mokhtari Masinaei, M. (2022). Damage Detection in Prestressed Concrete Slabs Using Wavelet Analysis of Vibration Responses in the Time Domain. Journal of Rehabilitation in Civil Engineering, 10(3), 37-63
https://doi.org/10.22075/jrce.2021.23385.1510

1. Introduction

Today, identifying features of structures is of vital importance in assessing their efficiency and estimating probable damages that may encounter [1–3]. Although many strengthening approaches are suggested and implied [4–9], these damages could result in sudden and unpredictable failures and bring about uncompensable financial and fatal damages. Hence, Structural Health Monitoring (SHM), especially the damage detection methods have been under focus of attention by researchers and engineers [10,11]. The Vibration-based structural health monitoring (VSHM) methods provide the possibility of performing effective testing and supervising of the structures for detection and locating the damages [12–14]. The most useful and extensive data on the structural health are the modal parameters like natural frequencies, mode shapes and modal damping [15]. These parameters are peculiar features of each structure and could be extracted from measured vibration responses. Where a structural system experiences unnormal conditions or is subjected to changes in the mass, stiffness or damping, the modal parameters values change with a specific trend, thus using these modal parameters one could detect structural damages [16–18]. Reviewing many research works [19–21] shows that the natural frequencies and damping ratios change with the excitation force and the environmental conditions surrounding the target structure [22]. Assessment of the previous research shows that the higher order mode shapes are more sensitive with respect to lower ones [23]. Although in the dynamical tests, access to higher order mode shapes is hard due to the limitation in creating vibration and boundary conditions. The limited structural mode shapes, limits the efficiency of vibration based damage detection methods. Furthermore, the traditional methods are based on the linear mode shapes of structures. On the other hand, damage detection methods are extended based on the time history analysis of structural responses measured for a structure. These methods do not require extracting the modal parameters as they directly take advantage from vibration data measured in the time domain.

Due to the complicated raw data measured in the time domain, which are normally nonlinear, their significant detection needs efficient tools like soft computing [24–31] or signal processing. Wavelet transform is one of the new methods developed for signal processing which is capable of signal description at different times (locations) and frequencies. The main advantage of wavelets is their capability of local analysis. On this basis, wavelets could detect some hidden aspects of signals like discontinuities and rupture points. The right application of wavelet analysis requires knowledge and experience, so that selecting a different family of wavelets or mother wavelet could greatly affect the analysis results and efficiency. In some research works, the wavelet transform of vibration data in the time domain is used for assessing structures and identifying damage in them. In the research performed by Law et al. [32], using the time history analysis of strain responses and accelerations with wavelet packet transform at different degrees of freedom, they proposed a method for damage detection in structures. The efficiency of their proposed method was confirmed by examining a full scale steel beam. Li et al. [33], by installing Piezoelectric transducers on different degrees of freedom of aluminum structures and sending Lamb waves on them and receiving

the corresponding responses, could detect the existing damages in these structures. They could detect the location and severity of the damages by applying wavelet transform on the received waves from the structure, and drawing contours of the wavelet coefficients. In a similar study, Vieira Filho et al. [34] applied wavelet analysis on Lamb waves received from Piezoelectric transducers installed on an aluminum plate and could detect the damage scenarios existing on it. Rauter and Lammering [35] analyzed lamb waves received from composite structures using the wavelet transform and assessed damages induced by impact on these structures. After investigating various mother wavelets, they reported Morlet mother wavelet as the most appropriate wavelet for their proposed method. Patel et al. [36] installed a number of sensors on different stories of a six-story reinforced concrete frame and by analyzing the difference in obtained accelerograms from these sensors in two states of damaged and undamaged structure using the wavelet transform, could detect the location of existing damages on the structure. They used the Gaussian wavelet transform coefficients as damage index. Qu et al. [37] proposed the adaptive wavelet transform, as the mean of short-time wavelet transforms with optimized time resolution in the time-frequency domain, for assessing debonding in concrete structures. The inputs of their proposed damage index are the impact echo responses at different degrees of freedom of the structure per two damaged and undamaged states. The results of the experimental assessment of rate of debonding between steel bars and surrounding concrete in a concrete slab show that the proposed method, in comparison to other methods that are based on the modal data analysis, is capable of detecting a higher number of cases. In the research performed by Naito and Blander [38], local vibration testing for detecting damage in the concrete elements has been used. They assessed the damages by creating vibration at different degrees of freedom in concrete elements and receiving vibration responses from them in two states of damaged and undamaged structure. The results revealed that the proposed method has a good capability in damage detection in experimental specimens of reinforced concrete beams and slabs.

Vibration responses in the time domain are more advantageous with respect to the modal data. However, few studies have dealt with damage detection in structures using analysis of response time histories. On the other hand, the prestressed concrete slabs as the common structural elements in recent years [39–45] are not considered as the benchmark of various damage detection techniques. To fulfil this gap, in this paper a number of different damage indices will be proposed. For this purpose, the time history of accelerations, due to applying the impact hammer force at different degrees of freedom in the numerical models of an experimental specimen of prestressed concrete slabs in two damaged and undamaged states, were considered as inputs for damage indices. The numerical models of prestressed concrete slabs have damage scenarios with different geometric shapes where some are located at the middle or at the corners of the slab. The proposed damage indices in this paper are obtained based on the acceleration time histories, maximum and area under diagram of detail coefficients of the wavelet transform using three wavelet families of Daubechies, Biorthogonal and Reverse Biorthogonal. To select the most appropriate damage index, their corresponding results are assessed and compared to each other.

2. Wavelet transform

Wavelet transform is one of the methods used for signal processing, which provides possibility of windowing with variable sizes. This type of transform has improved signal analysis with local changes by focusing on the short time intervals for high frequency components and focusing on long time intervals for low frequency components [46–48]. The wavelet transform uses the scale instead of frequency which is inversely proportional with frequency. In the wavelet transform, each signal could be decomposed into a set of functions which are derived from a specific wavelet called mother wavelet $\psi(x)$ [49–51]. In wavelet transform, the function $\psi(t,a,b)$ is the scaled and translated version of mother wavelet:

$$\psi(t,s,b)=\frac{1}{\sqrt{s}}\psi\left(\frac{t-b}{s}\right) \quad (1)$$

In Eq. (1), s is the scale parameter and b is the translation parameter. The wavelet transform parameters and its coefficients are the scale and translation. In fact scaling of a wavelet means its compressing or stretching. On the other hand translation of a wavelet means delaying its start [49,52]. Continuous wavelet transform (CWT) is the sum of the signal multiplied by the scaled and translated wavelet function $\psi(t,a,b)$:

$$CWT(s,b)=\int_{-\infty}^{\infty} f(t)\cdot\psi(t,s,b)dt \quad (2)$$

Eq. (2) yields the wavelet coefficients which are a function of scale and position. These coefficients show the relation and similarity between the wavelet function and the original signal. The higher the coefficients are, the higher is the similarity and the result depends upon the shape of selected wavelet.

Computing coefficients per any scale generates too much data. In order to reduce the number of these analytical data, the scales and positions are defined based on powers of 2 which are called dyadic scales and positions. This type of analysis is called Discrete Wavelet Transform (DWT). Implementing this type of analysis using filters was developed by Mallat in 1999 [46], which is now called as fast wavelet transform. This transform could be imagined as a toolbox where the input is the original signal and its outputs are the wavelet coefficients. In this transform, the wavelet function is defined as follows:

$$\psi_{j,k}(t)=\frac{1}{\sqrt{2^j}}\psi\left(\frac{t-2^j k}{2^j}\right)=2^{-j/2}\,\psi(2^{-j}t-k) \quad (3)$$

In Eq. (3), j is the level of decomposition, t is the time and 2^j is the scale. Eq. (4) shows how the discrete wavelet transform coefficients are calculated as sum of the signal $f(t)$ multiplied by the scaled and translated wavelet function $\psi_{j,k}(t)$:

$$DWT(j,k)=\int_{-\infty}^{\infty} f(t)\cdot\psi_{j,k}(t)dt \quad (4)$$

In the discrete wavelet transform, the original signal passes through the highpass and lowpass filters. Filters are linear operators independent of time. The lowpass filter smoothes the bumps in a signal. The highpass filter shows the signal bumps and removes or reduces the smoothed portions [19,53]. The high scale low frequency components of a signal are called approximation coefficients and the low scale high frequency components of it are called detail coefficients. The wavelet transform, by filtering the original signal, provides the possibility of identifying these components. The decomposition process could be continued by sequential decomposition of the approximation coefficients. In this procedure, the original

signal is divided into a great number of components which is called wavelet decomposition tree. The wavelet decomposition tree contains valuable information. At each level of this tree, one could access the signal approximation and detail coefficients. As damage in a structure is sudden and a phenomenon with high frequency, detail coefficients of input signal used in order to detect damages.

Contrary to the continuous wavelet transform (CWT), which uses only the wavelet function $\psi(t)$, in the discrete wavelet transform (DWT) in addition to the wavelet function, the scaling function $\emptyset(x)$ is also used. Wavelet and scaling functions are related to lowpass and highpass filters, respectively. The scaling function is very much similar to the wavelet function. In fact, the wavelet function provides the detail coefficients, and the scaling function provides the approximation coefficients of a decomposed signal. Among the wavelet functions only the orthogonal wavelets possess scaling function [54,55].

Up to now, various wavelet families have been presented for signal processing which could be classified according to their different characteristics [46]. The Gaussian, Mexican hat, Shannon and Morlet families of wavelets have an explicit relation for the wavelet function,ψ. These wavelets do not possess scaling function, $\emptyset$. Therefore, there is no possibility of discrete wavelet transform for them and they could not be reconstructed by discretion. Analysis of these wavelets is limited to the continuous wavelet transform. The Haar, Daubechies and Coiflet wavelets do not possess an explicit relation for the wavelet function, ψ. In these wavelets due to the presence of scaling function,$\emptyset$ one could also use the discrete wavelet function. They have a small regularity and are not symmetric. The Biorthogonal wavelets and their inverse, named Reverse Biorthogonal wavelets are another class of wavelets that are symmetric and precise reconstruction of wavelets is possible in them. Also they have two different wavelets and scaling functions. As an instance, Figs. 1, 2 and 3 show the wavelet functions $(\psi(x))$ and scaling functions $((\emptyset))$ of each mother wavelet for Daubechies, Biorthogonal and Reverse Biorthogonal wavelet families, respectively.

The way that an appropriate and optimal wavelet is selected for processing the signal of a specific phenomenon is dependent upon the wavelet characteristics and the intended signal. In most cases, one could not be fully sure which wavelet is good to use and it is done by trial and error. In this paper, different mother wavelets of Daubechies, Biorthogonal and Reverse Biorthogonal wavelet families has been used for damage detection.

3. Numerical models

3.1. Models verification

In this paper, experimental specimens of prestressed concrete slabs in Pahlevan Mosavari study [56] has been used in order to build up the numerical models. In that study, the modal parameters of a number of prestressed concrete slab experimental specimens with dimensions of 160cm × 60cm and thicknesses of 10cm, 15cm and 20cm were obtained using the modal testing. In order to construct the experimental specimens, the concrete with 30MPa compressive strength and steel cables with 250MPa yield strength, 4.97mm diameter and cover of 25mm were considered.

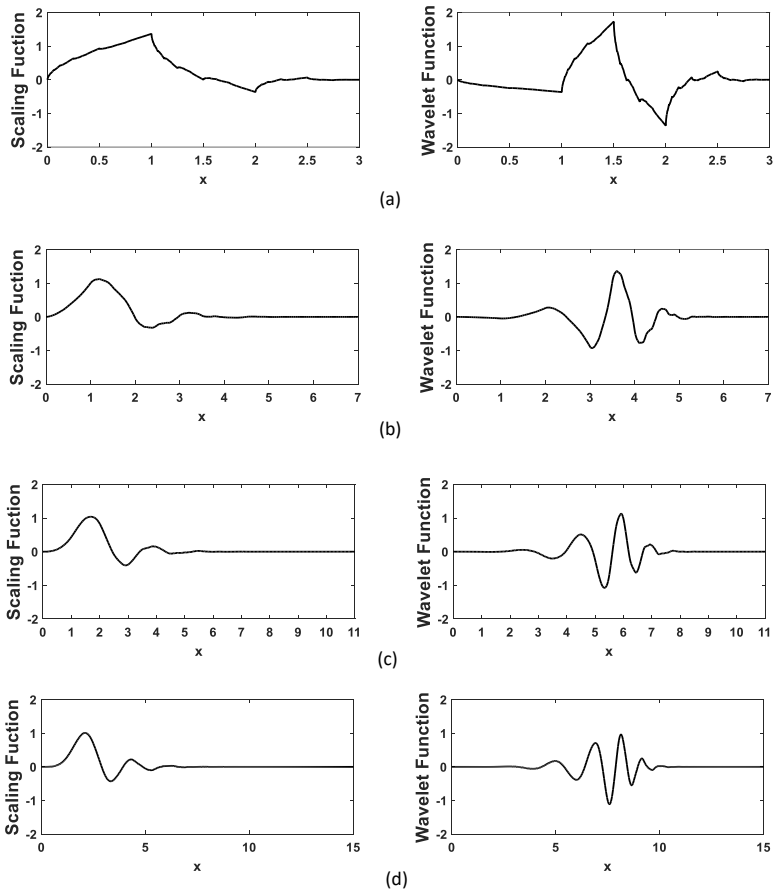

Fig. 1. Daubechies family of wavelets with different mother wavelets: a) db2; b) db4; c) db6 and d) db8.

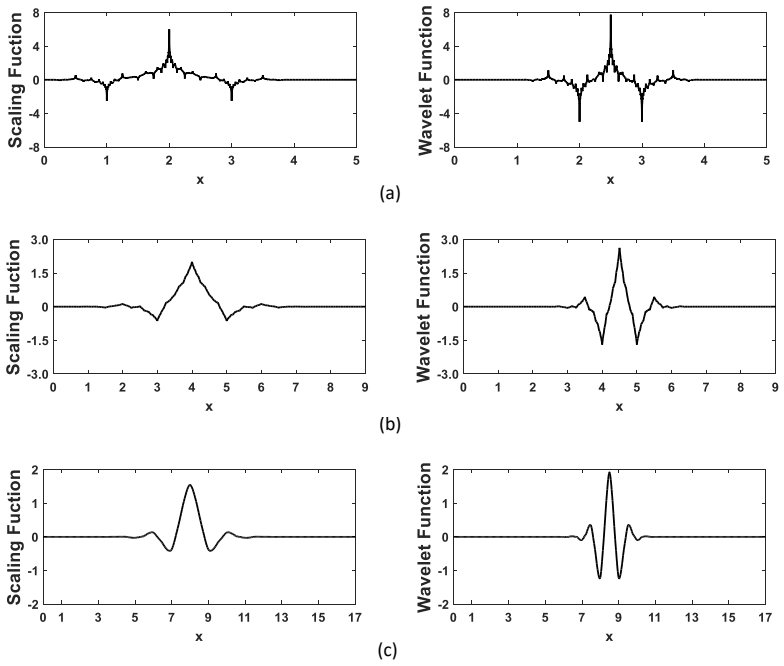

Fig. 2. Biorthogonal family of wavelets with different mother wavelets: a) bior2.2; b) bior2.4 and c) bior2.8.

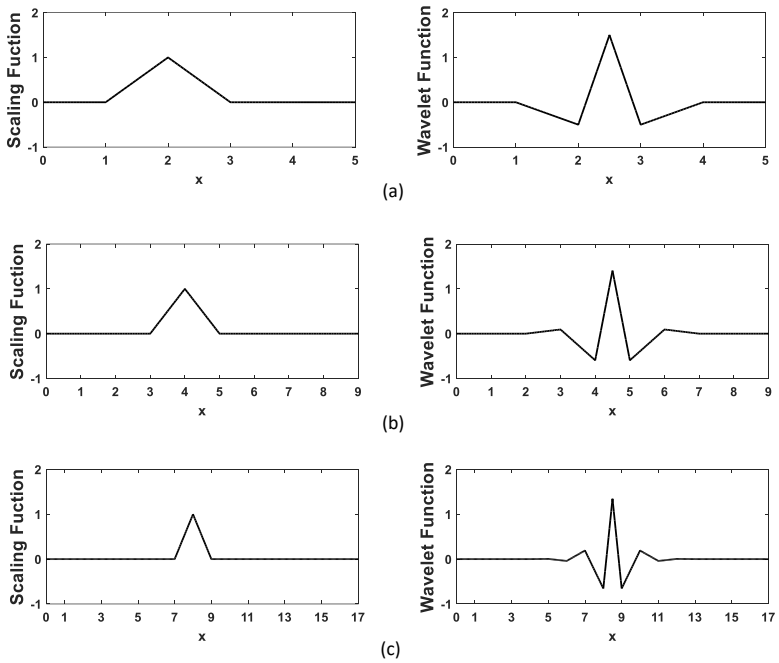

Fig. 3. Reverse Biorthogonal family of wavelets with different mother wavelets: a) rbio2.2; b) rbio2.4 and c) rbio2.8.

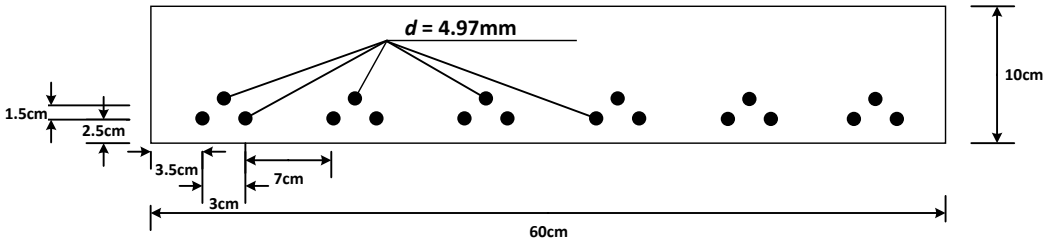

Fig. 4. Cross sectional view of prestressed concrete slabs [56].

The mechanical properties of the used materials is reported in Table 1 and Fig. 4 shows the cross sectional view of the experimental prestressed concrete slab with 10cm thickness.

Table 1. Mechanical properties of materials in experimental prestressed concrete slab specimens [56]

Materials	Density (kg/m^3)	Elastic modulus (GPa)	Poisson's ratio
Concrete	2200	23.5	0.2
Steel	8750	200	0.3

Pahlevan Mosavari [56] conducted modal testing to obtain the modal parameters of the experimental prestressed concrete slab specimens. For that purpose, a net of nodes with 15cm intervals on the upper surface of each specimen were considered as its degree of freedoms. As shown in Fig. 5, in order to reduce the boundary condition effects, each specimen was hanged by a number of elastic bands. By applying an impact hammer at each degree of freedom and measuring the inflicted impact and the responses received fom the accelerometer which was installed at the middle of the slab, the natural frequencies and mode shapes of the specimens were calculated using the frequency response functions (FRFs).

Fig. 5. Hanged position of the prestressed concrete slab specimen for performing modal testing [56].

In this paper, one of the specimens of prestressed concrete slabs reported in the Pahlevan Mosavari study [56] with 10cm thickness is selected and modeled in ABAQUS software. The plastic damage model in the ABAQUS software library has been used to model concrete materials. In this model, which was first proposed in the research by Lubliner et al. [57], the two modes of cracking in tension and softening in compression are assumed for the concrete materials. As a result, after concrete cracking in tension or concrete crushing in compression, per any point of the stress-strain diagram, a certain amount of damage is assumed. The assumption of Onate et al. [58] was utilized, in order to obtain the tensile and compressive amounts of damages. On this basis, before the stress value in the material reaches the tensile and compressive strength values, the amount of damage due to tension and uniaxial compression is zero. By entering the strain softening region (extension of tensile cracking or crushing in concrete), the tensile and compressive damage value increases. On the other hand, it is considered that the prestressed bars behave like a truss and a full contact between bars and concrete is assumed. In the prestressed concrete slab models, the steel material is considered to behave bilinear in accordance with the properties presented in Table 1. The C3D20 element with 20 nodes, where each node has three components of translation degrees of freedom, used for meshing of the numerical models. This type of element is used for nonlinear analyses including the contact, large deformations, plasticity and damage analysis [59]. Moreover, the truss element T3D3 has been incorporated for steel bars. To achieve a suitable meshing with natural frequencies close to the experimental results, various meshing attempts were performed and the most optimal one was adopted. The dimensions of optimal meshing were obtained equal to 20mm size cubics as shown in Fig. 6.

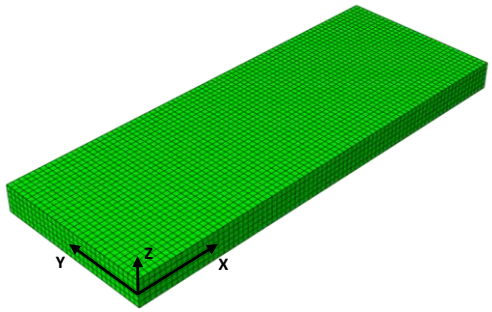

Fig. 6. Optimal meshing of the numerical models.

In order to simulate the prestressing action, initial stresses were defined in steel cables. The initial stress for the upper and lower rebars (Fig. 4) is taken equal to 7156 kg/cm^2 and 9600 kg/cm^2, respectively. As shown in Fig. 7, applying the initial stresses induced a negative deflection in the prestressed concrete slab specimens.

Fig. 8 shows the first three mode shapes in the prestressed concrete slab model. In Table 2, the natural frequencies in the numerical model are compared with the corresponding results obtained from modal testing in the Pahlevan Mosavari research work [56].

Table 2. Comparison of natural frequencies between numerical model and experimental specimen.

Shape Modes	Natural frequencies (Hz)		Error (%)
	Experimental Specimen [56]	Numerical Model	
First Mode	125.1	128.4	2.64
Second Mode	201.8	207.9	3.02
Third Mode	341.2	346.2	1.47

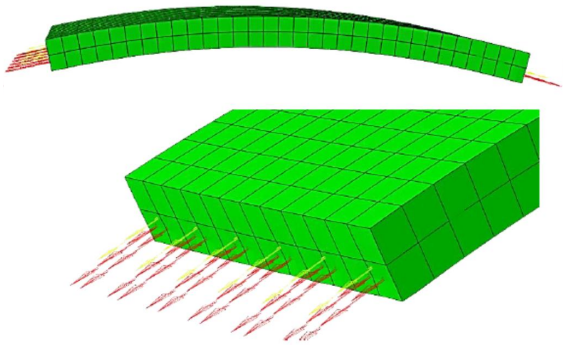

Fig. 7. Negative deflection resulted from simulation of prestressing action in the concrete slab models.

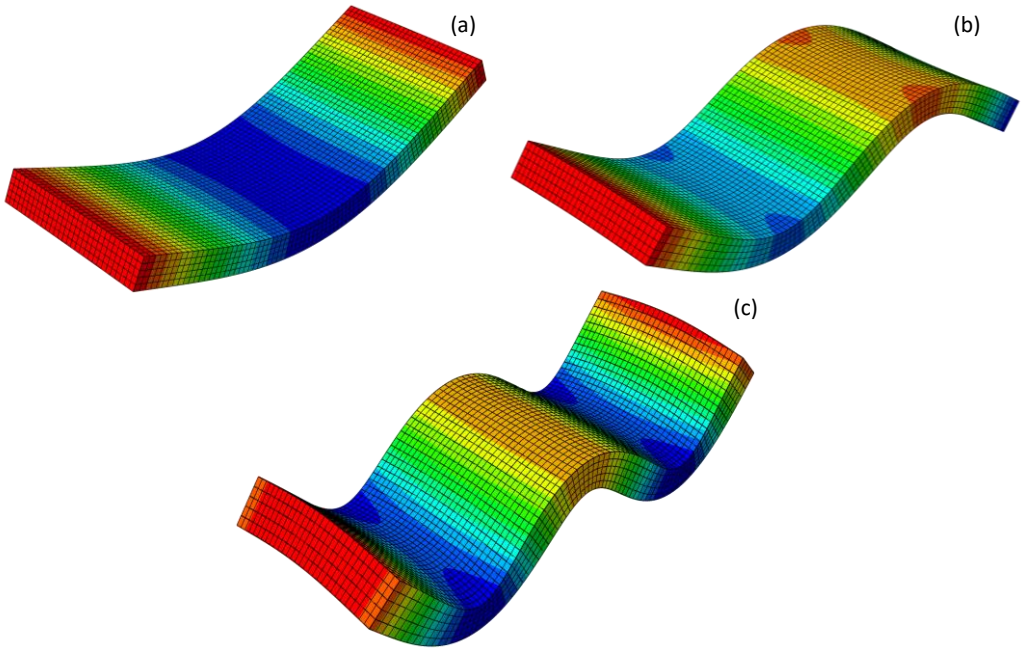

Fig. 8. a) first; b) second and c) third mode shape of the prestressed concrete slab model.

As seen in Table 2, the natural frequencies of the numerical model in this paper are appropriately compatible with those obtained by the modal testing on the prestressed concrete slab specimens in the Pahlevan Mosavari research work [56]. The negligible difference between the frequencies in the numerical model and those in the experimental specimens could be attributed to inability in providing full hanging condition in the experimental conditions and the results show that the numerical model could be used confidentially.

3.2. Damage scenarios

After being ensured regarding accuracy of the built numerical model in ABAQUS software in the previous section, some damage scenarios with different shapes and at different locations are created in a number of prestressed concrete slab models. Contrary to the previous section, where the prestressed concrete slabs was modelled in suspended condition for compatibility with modal testing, in this section of the paper, the edges of lower surface of the slabs are situated on hinged supports. As shown in Fig. 9, 75

different degrees of freedom are considered in the numerical models of the prestressed concrete slabs.

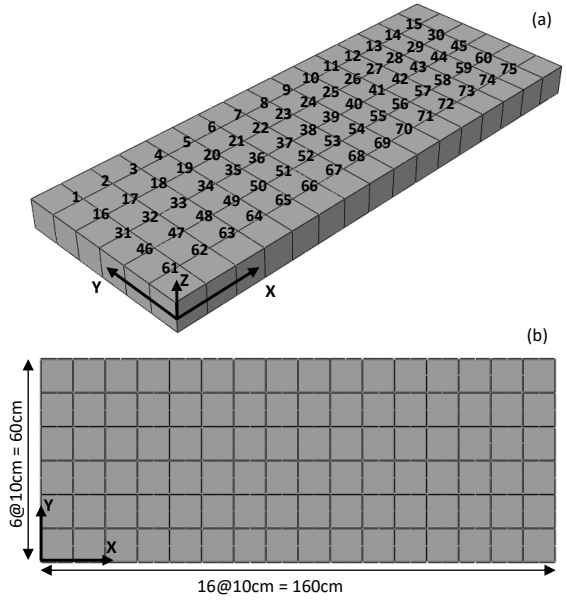

Fig. 9. Degrees of freedom in presstressed concrete slab models: a) 3D view; b) 2D view.

In order to assess the features of numerical models, in this paper, modal testing has been simulated on the prestressed concrete slabs using the impact hammer. In the modal tests, after dividing the structure into different degrees of freedom, to identify its mechanical properties, a number of impacts are applied on each degree of freedom using the hammer. The mean value of forces exerted on each degree of freedom by the impact hammer is calculated and simultaneously a sensor is used for receiving the accelerations obtained as the result of applied impacts. Given the input forces and output accelerations from the structure, its mechanical properties could be obtained. In the modal testing, instead of applying impact hammer at each degree of freedom and get the corresponding responses from a sensor fixed at a specific point, an impact could be applied on a specific degree of freedom to find the resulted accelerations on each degree of freedom. In this research, the second case is applied for identification of mechanical properties of the numerical models pertaining to the prestressed concrete slabs. For this purpose, the force exerted by the impact hammer from the Pappalardo and Guida research [60] is utilized as shown in Fig. 10. The impact hammer force is applied at No. 25 degree of freedom with 2D geometric coordinates of (100, 40) and the resulted accelerations are obtained per different degrees of freedom.

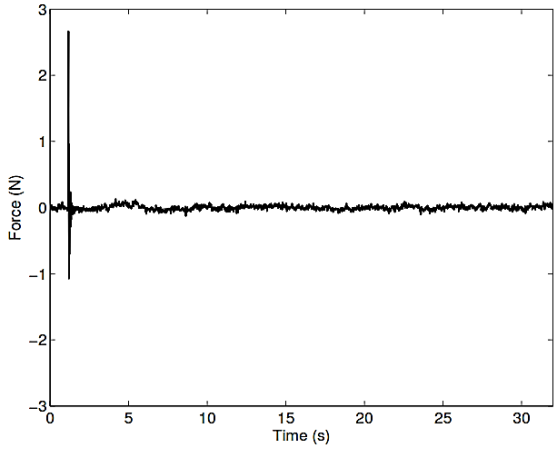

Fig. 10. Diagram of impact hammer force in the Pappalardo and Guida research [60].

The damage scenarios in this paper are assumed as three damge type with different geometric shapes at two different locations on numerical models of prestressed concrete slabs. As shown in Fig. 11, Transverse, longitudinal and inclined slots with 60mm length, 10mm width and depth of 20mm were considered as different damage types which were created at middle (No. 38 degree of freedom with 2D geometric coordinates of (80, 30)) and corner (No. 59 degree of freedom with 2D geometric coordinates of (140, 20)) of the lower surface of the numerical models of prestressed concrete slabs.

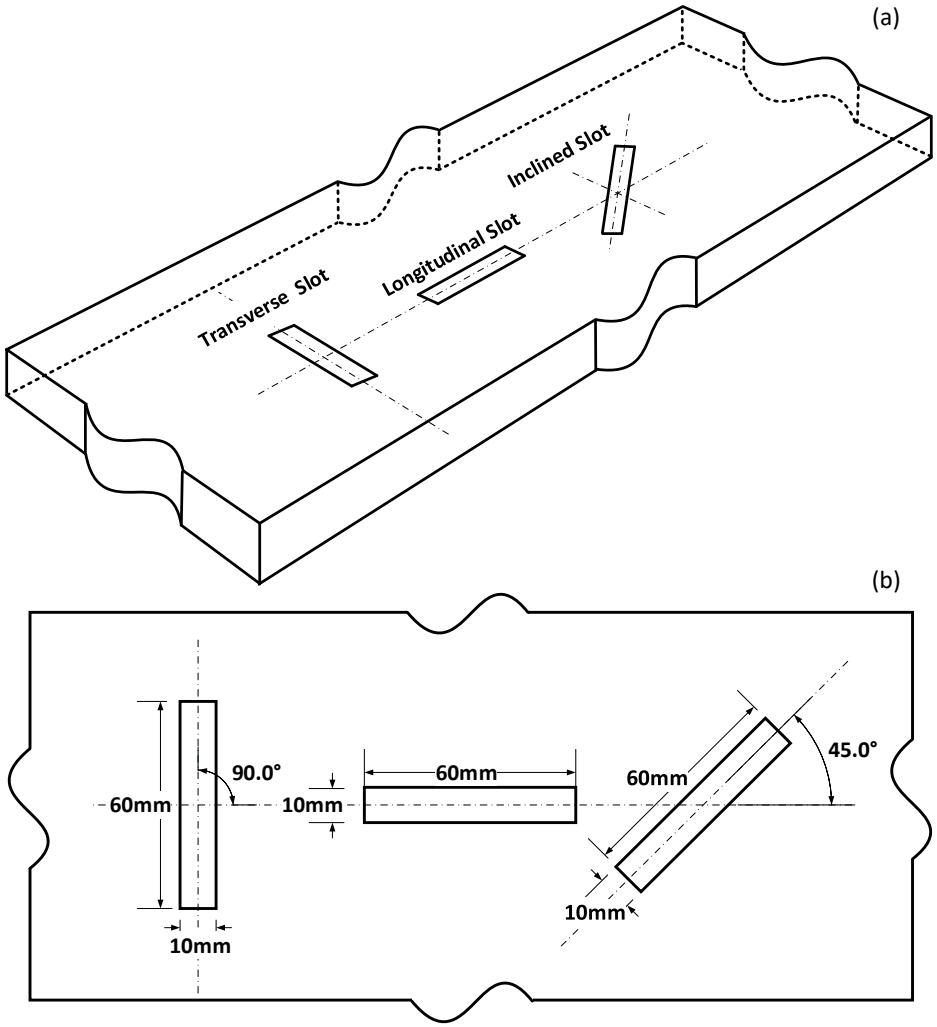

Fig. 11. Transverse, longitudinal and inclined slots as different damage types: a) 3D view; b) 2D view.

The numerical models including different damage scenarios were labelled according to the notation of S_DL_DT, in which, S indicates the single damage scenario, DL represents the dmage location (M and C for middle and center, respectively) and DT demonstrates the damage type (TS, LS and IS for Transverse, longitudinal and inclined slot, respectively). Based on the damage locations, numerical models were classified into two S_M (middle) and S_C (center) groups. The geometric properties of damage scenarios in numerical models of prestressed concrete slabs are reported in Table 3.

Table 3. Geometric properties of damage scenarios in the numerical models of prestressed concrete slabs

Damage Scenario		Damage Location			Damage Type
Group	Name	Location	Degree of Freedom	2D Coordinate (X, Y)(cm)	
S_M	S_M_TS	Middle	No. 38	(80, 30)	Transverse Slot
	S_M_LS				Longitudinal Slot
	S_M_IS				Inclined Slot
S_C	S_C_TS	Corner	No. 59	(140, 20)	Transverse Slot
	S_C_LS				Longitudinal Slot
	S_C_IS				Inclined Slot

4. Damage localization

In this paper, a number of different damage indices have been proposed for identifying the location of damages. The inputs for all these indices are the accelerations time histories per different degrees of freedom of prestressed concrete slabs in two states of damaged and undamaged model. For each degree of freedom in the prestressed concrete slabs (N_i), the proposed damage index *DI_SA* is obtained based on the difference between the areas under the diagram of accelerations time histories corresponding to two states of damaged and undamaged model:

$$\left(DI\_SA\right)_{N_i} = \frac{\left(SA_D - SA_U\right)_{N_i}}{\max\left(\left(SA_U\right)_{N_i}\right)} \quad (5)$$

In Eq. (5), SA_D and SA_U denotes the area under diagram of acceleration time histories at degree of freedom N_i, in the prestressed concrete slab for two states of damaged and undamaged model, respectively. by conducting trial and error analyses, the Daubechies, Biorthogonal and Reverse Biorthogonal family were selected as the best wavelet families. Applying each of the mother wavelets db2, db4, db6 and db8 from Daubechies wavelet family, bior2.2, bior2.4 and bior2.8 from Biorthogonal wavelet family and rbio2.2, rbio2.4 and rbio2.8 from Reverse Biorthogonal family on the accelerations time histories obtained from each degree of freedom in the prestressed concrete slab models (N_i), and per two damaged and undamaged states, the proposed damage indices of *DI_MW* and *DI_SW* are obtained by Eq. (6) and Eq. (7) based on the difference between maximum values, and area under diagram of corresponding detail coefficients, respectively:

$$\left(DI\_MW\right)_{N_i} = \frac{\left(MW_D - MW_U\right)_{N_i}}{\max\left(\left(MW_U\right)_{N_i}\right)} \quad (6)$$

$$\left(DI\_SW\right)_{N_i} = \frac{\left(SW_D - SW_U\right)_{N_i}}{\max\left(\left(SW_U\right)_{N_i}\right)} \quad (7)$$

In Eq. (6) and Eq. (7), MW_D and MW_U denote the maximum detail coefficients and similarly, SW_D and SW_U represent the areas under diagram of detail coefficients obtained from applying wavelet transform on the accelerations time histories of damaged and undamaged models, respectively. The results obtained from applying each of the proposed damage indices *DI_SA*, *DI_MW* and *DI_SW* on all numerical models are reported in Table 4, in which, the damage identification results were classified in three different categories including well detected (✓✓), approximately detected (✗✓) and not detected (✗✗).

Table 4 shows that, the proposed damage index *DI_SA* could only detect damages in S_M_LS, S_C_LS and S_C_IS numerical models. On the other hand, for the proposed damage index *DI_MW*, db4 from Daubechies wavelet family, bior2.2 from Biorthogonal wavelet family and rbio2.4 from Reverse Biorthogonal wavelet family had the best results in detecting damage scenarios. Also for the proposed damage index *DI_SW*, db2 from Daubechies wavelet family, bior2.2 from Biorthogonal wavelet family and rbio2.2 from Reverse Biorthogonal wavelet family had well capability in detecting damages with respect to other mother wavelets.

Table 4. Results of applying the proposed damage indices on the numerical models

Damage Indices			S_M_TS	S_M_LS	S_M_IS	S_C_TS	S_C_LS	S_C_IS
DI_SA			✗✗	✗✓	✗✗	✗✗	✗✓	✗✓
DI_MW	Daubechies	db2	✗✓	✗✗	✗✓	✗✗	✗✗	✗✗
		db4	✗✓	✗✓	✗✓	✗✓	✗✗	✗✗
		db6	✗✗	✗✗	✗✗	✗✗	✗✗	✗✗
		db8	✗✓	✗✗	✗✓	✗✗	✗✗	✗✗
	Biorthogonal	**bior2.2**	✗✗	✗✗	✗✓	✗✗	✗✗	✗✗
		bior2.4	✗✗	✗✗	✗✗	✗✗	✗✗	✗✗
		bior2.8	✗✗	✗✗	✗✗	✗✗	✗✗	✗✗
	Reverse Biorthogonal	rbio2.2	✗✗	✗✗	✗✗	✗✗	✗✗	✗✗
		rbio2.4	✗✓	✗✗	✗✓	✗✗	✗✗	✗✗
		rbio2.8	✗✗	✗✗	✗✗	✗✗	✗✗	✗✗
DI_SW	Daubechies	**db2**	✓✓	✓✓	✓✓	✓✓	✓✓	✓✓
		db4	✗✓	✗✗	✗✓	✗✓	✗✗	✗✗
		db6	✗✓	✗✗	✗✓	✗✗	✗✗	✗✗
		db8	✗✓	✗✗	✗✓	✗✗	✗✗	✗✗
	Biorthogonal	**bior2.2**	✗✓	✗✗	✗✓	✗✓	✗✓	✗✓
		bior2.4	✗✓	✗✗	✗✓	✗✗	✗✗	✗✗
		bior2.8	✗✓	✗✗	✗✓	✗✗	✗✗	✗✗
	Reverse Biorthogonal	**rbio2.2**	✗✓	✗✓	✗✓	✓✓	✓✓	✓✓
		rbio2.4	✗✓	✗✗	✗✓	✗✗	✗✗	✗✗
		rbio2.8	✗✓	✗✗	✗✓	✗✗	✗✗	✗✗

In some research works [61,62], it is recommended that for better presenting the location of detected damages using the damage indices, a threshold be introduced based on the statistical data of the index values. In this paper, also the following damage threshold is used for a better presentation of damage location [63]:

$$Tr_{\alpha} = \mu + Z_{\alpha}\left(\frac{\sigma}{\sqrt{n}}\right) \quad (8)$$

In Eq. (8), μ and σ are the mean and standard deviation values of damage index, respectively. In addition, Z_{α} is the normal distribution with the mean and standard deviation values of zero and one, respectively, and cumulative probability of 100(1- α)(%). In this paper, the threshold value (Tr_{α}) is calculated with 95% margin of safety (α = 0.05). The Tr_{α} value could be used as a threshold for identifying the location and removing irregularities of the damage index. The degrees of freedom where the damage index exceeds the threshold value are accounted as damaged degrees of freedom. The way the threshold value is applied on the damage index is illustrated in Fig. 12.

The corresponding results of the proposed damage index *DI_SA* after applying the damage threshold (Tr_{α}) on all numerical models are given in Fig. 13.

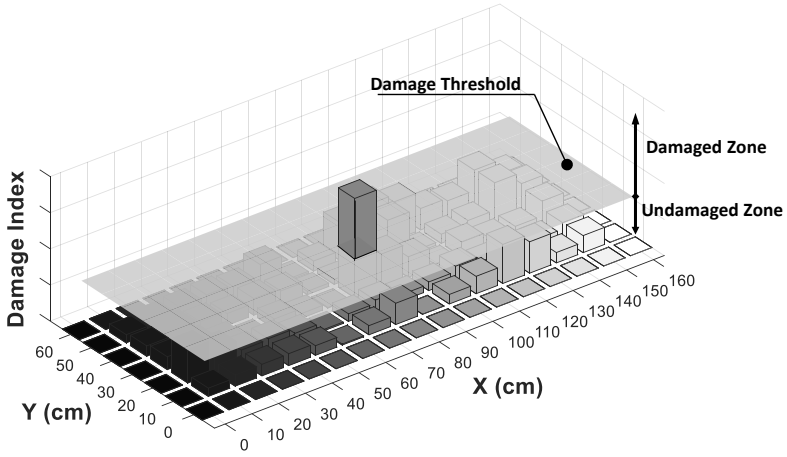

Fig. 12. Applying the threshold value (Tr_{α}) on damage index.

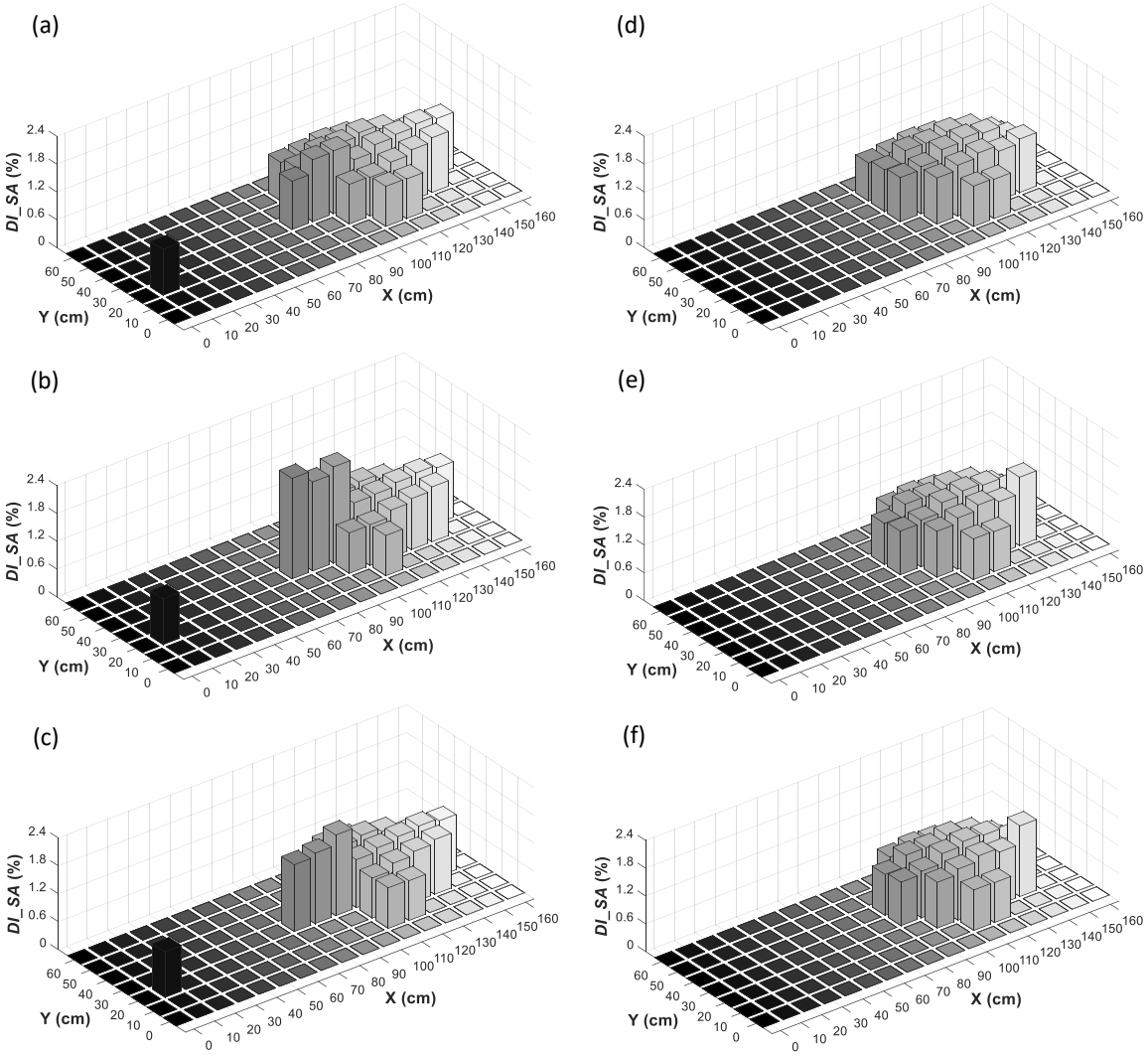

Fig.13. Results of the proposed damage index *DI_SA* in the numerical models: a) S_M_TS; b) S_M_LS; c) S_M_IS; d) S_C_TS; e) S_C_LS and f) S_C_IS.

Fig.13 shows that according to Table 4, the proposed damage index *DI_SA* had a rough success in detecting location of the damage scenarios in S_M_LS, S_C_LS and S_C_IS numerical models. However, it was not significantly capable of detecting location of the damage scenarios in S_M_TS, S_M_IS and S_C_TS numerical models. Hence, in this research, to improve the method of detecting damage scenarios, the wavelet transform was used in the damage indices *DI_MW* and *DI_SW*.

According to Table 4, the results of trial and error method for selection of mother wavelet show that for the proposed damage index *DI_MW*, db4 from the wavelet family Daubechies, bior2.2 from the wavelet family Biorthogonal, and rbio2.4 from the wavelet family Reverse Biorthogonal exhibit better efficiency in detecting the damages. The results of proposed damage index *DI_MW* after applying the damage threshold (Tr_α) in all numerical models with the mother wavelet db4 are shown in Fig. 14.

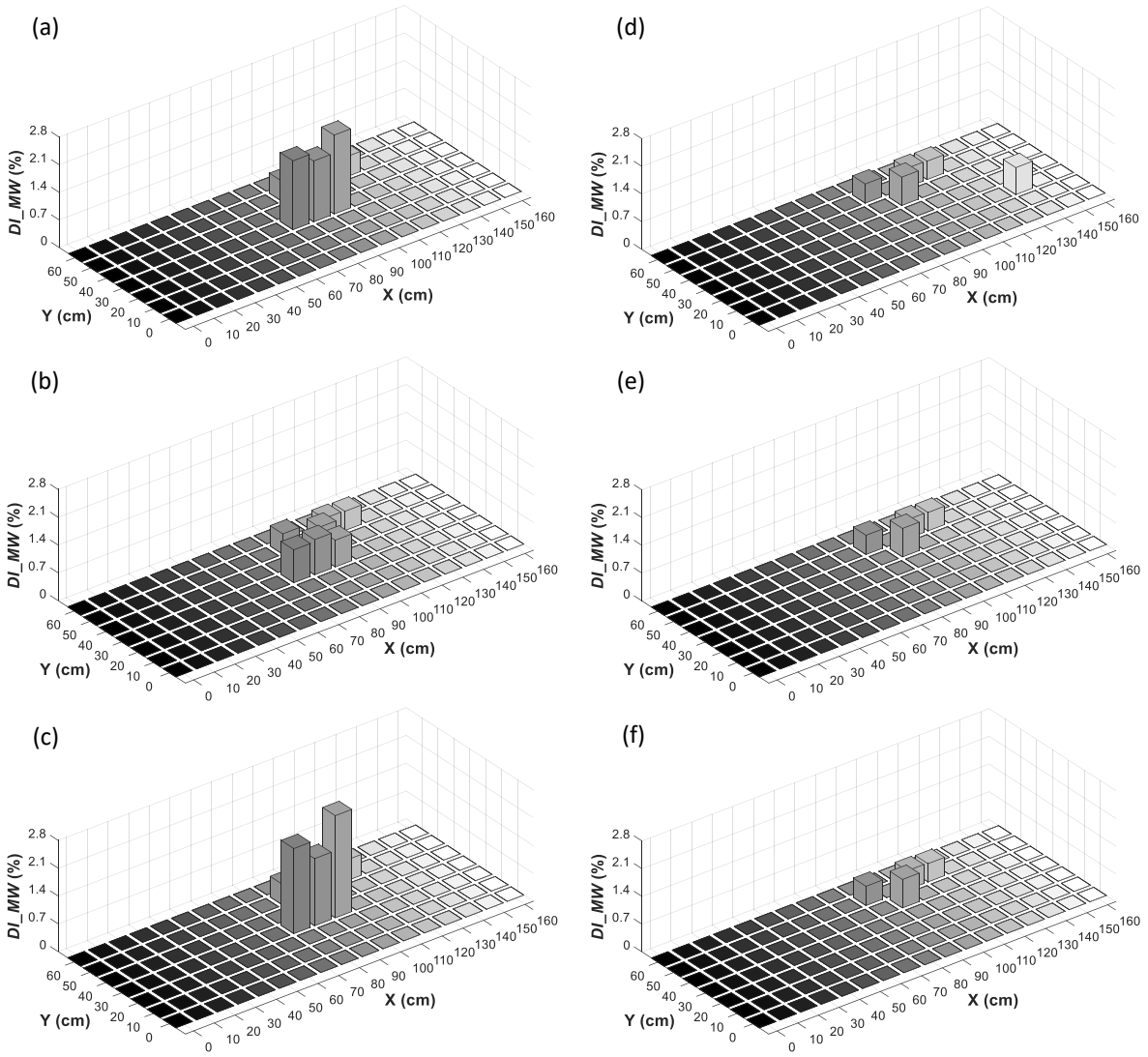

Fig. 14. Results of the proposed damage index *DI_MW* with mother wavelet db4 in the numerical models: a) S_M_TS; b) S_M_LS; c) S_M_IS; d) S_C_TS; e) S_C_LS and f) S_C_IS.

Fig.14 shows that according to what is reported in Table 4, the mother wavelet db4 used in the proposed damage index *DI_MW* for the numerical models S_M_TS, S_M_LS, S_M_IS, and S_C_TS, was somehow successful in detecting the location of damage scenarios. On the other hand, damages in S_C_LS and S_C_IS numerical models, using the proposed damage index *DI_MW* with mother wavelet db4 were not detected in any way. Fig. 15 shows the results of proposed damage index *DI_MW* after applying the damage threshold (Tr_α) with the mother wavelet bior2.2 in all numerical models.

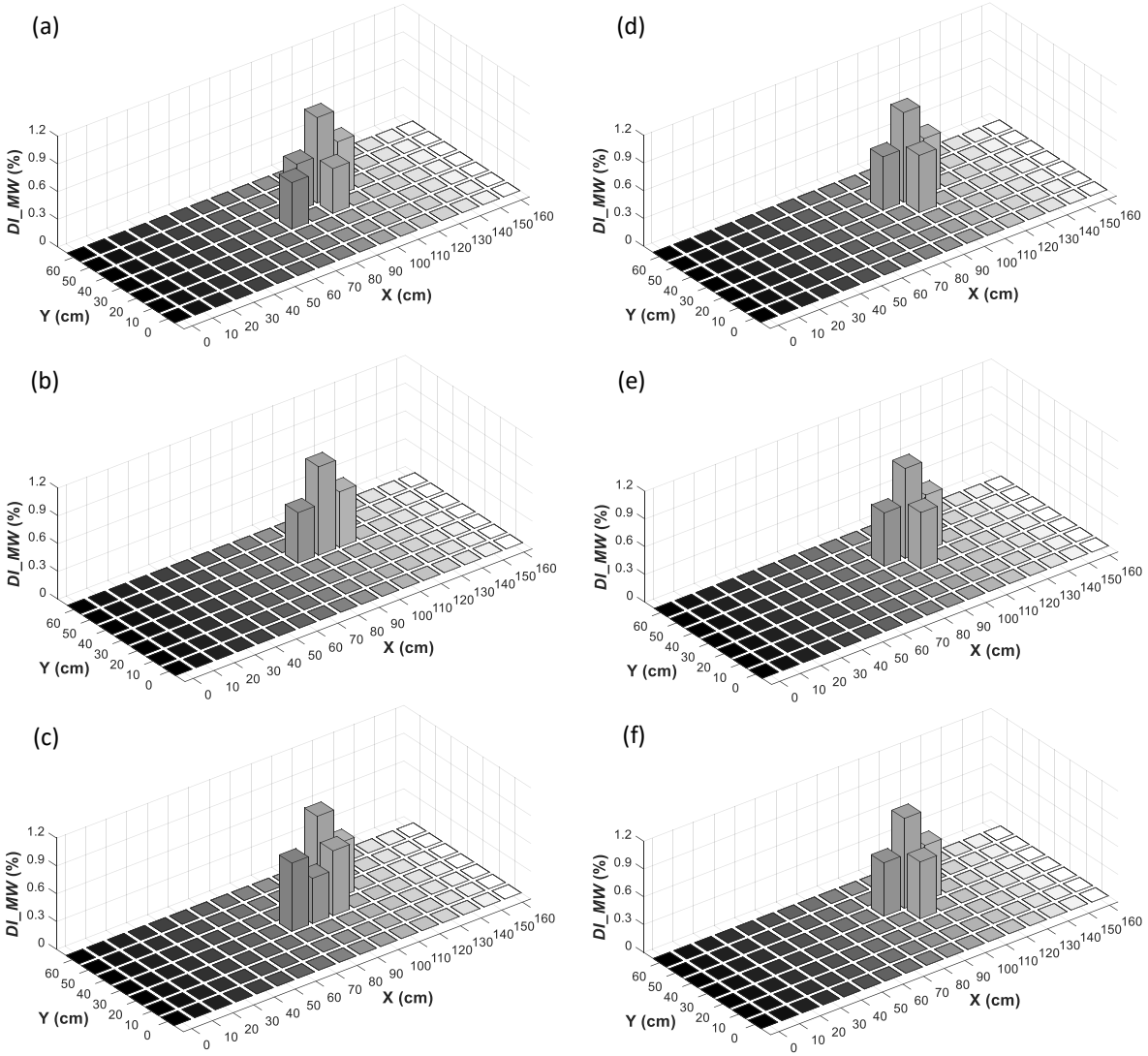

Fig.15. Results of the proposed damage index *DI_MW* with mother wavelet bior2.2 in the numerical models: a) S_M_TS; b) S_M_LS; c) S_M_IS; d) S_C_TS; e) S_C_LS and f) S_C_IS.

According to the results given in Fig. 15 and Table 4, the proposed damage index *DI_MW* with the mother wavelet bior2.2 has somehow estimated the location of damage in S_M_IS numerical model and was not successful in detecting damage in other numerical models. The results of using the mother wavelet rbio2.2 in the damage index *DI_MW* after applying the damage threshold (Tr_α) in all numerical models are shown in

Fig. 16. As seen in Fig. 16, the proposed damage index *DI_MW* using the mother wavelet rbio2.4 has been somehow successful in detecting damage location just in S_M_TS and S_M_IS numerical models.

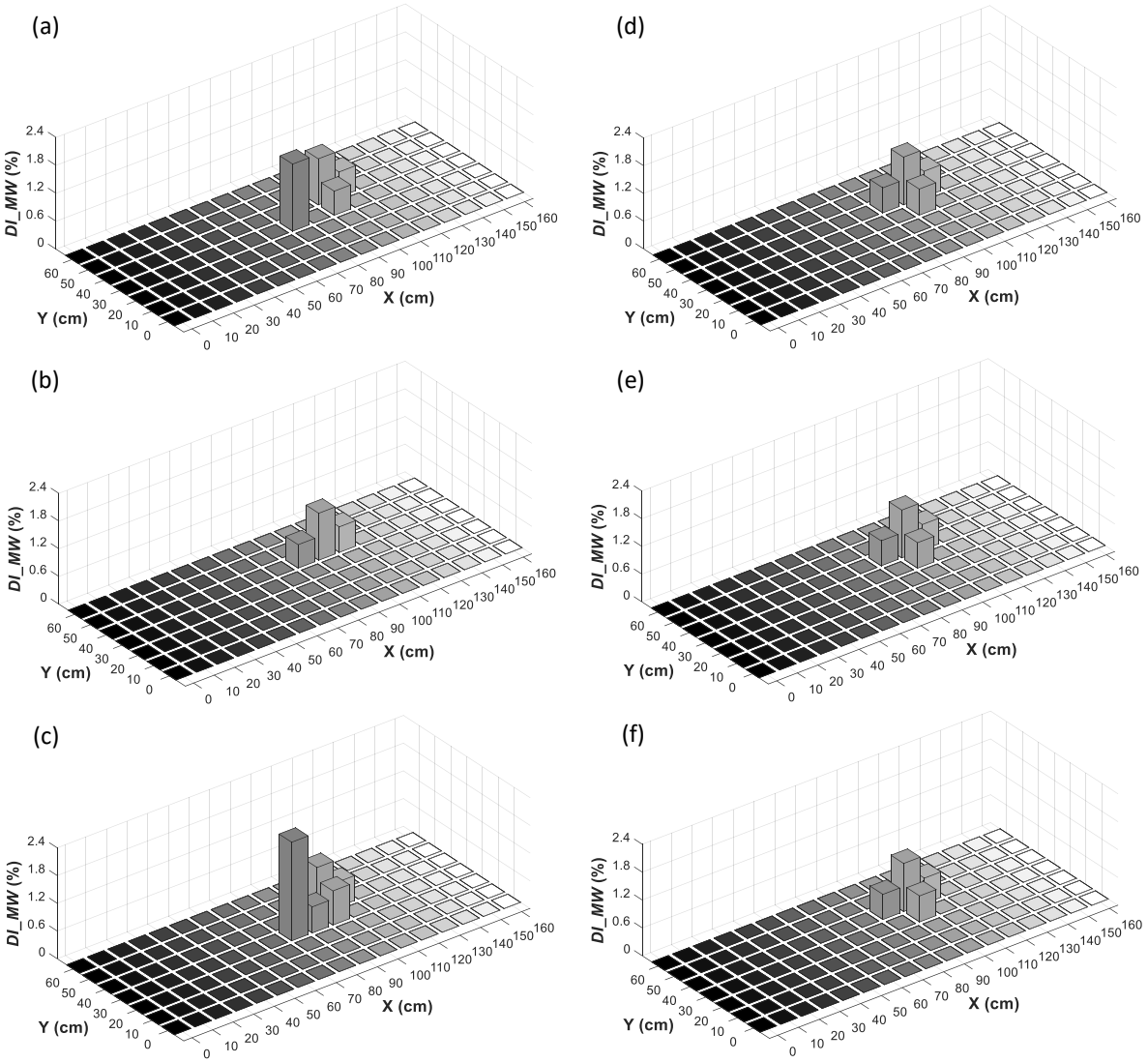

Fig.16. Results of the proposed damage index *DI_MW* with mother wavelet rbio2.4 in the numerical models: a) S_M_TS; b) S_M_LS; c) S_M_IS; d) S_C_TS; e) S_C_LS and f) S_C_IS.

Generally, reviewing Figs. 13 to 16, it could be stated that the damage index *DI_MW*, which is calculated by difference between the maximum values of detail coefficients of the wavelet transform applied on the acceleration time histories at different degrees of freedom, is not suitable for detecting the damage location in the prestressed concrete slabs models. Consequently, in the following of the paper, instead of using the maximum values of the detail coefficients, the *DI_SW* damage index is proposed based on the area under the detail coefficients diagram and its corresponding results will be compared to those of the *DI_MW* damage index.

The results of proposed damage index *DI_SW* after applying the damage threshold (Tr_α) using the mother wavelet db2 in all numerical models are presented in Fig. 17.

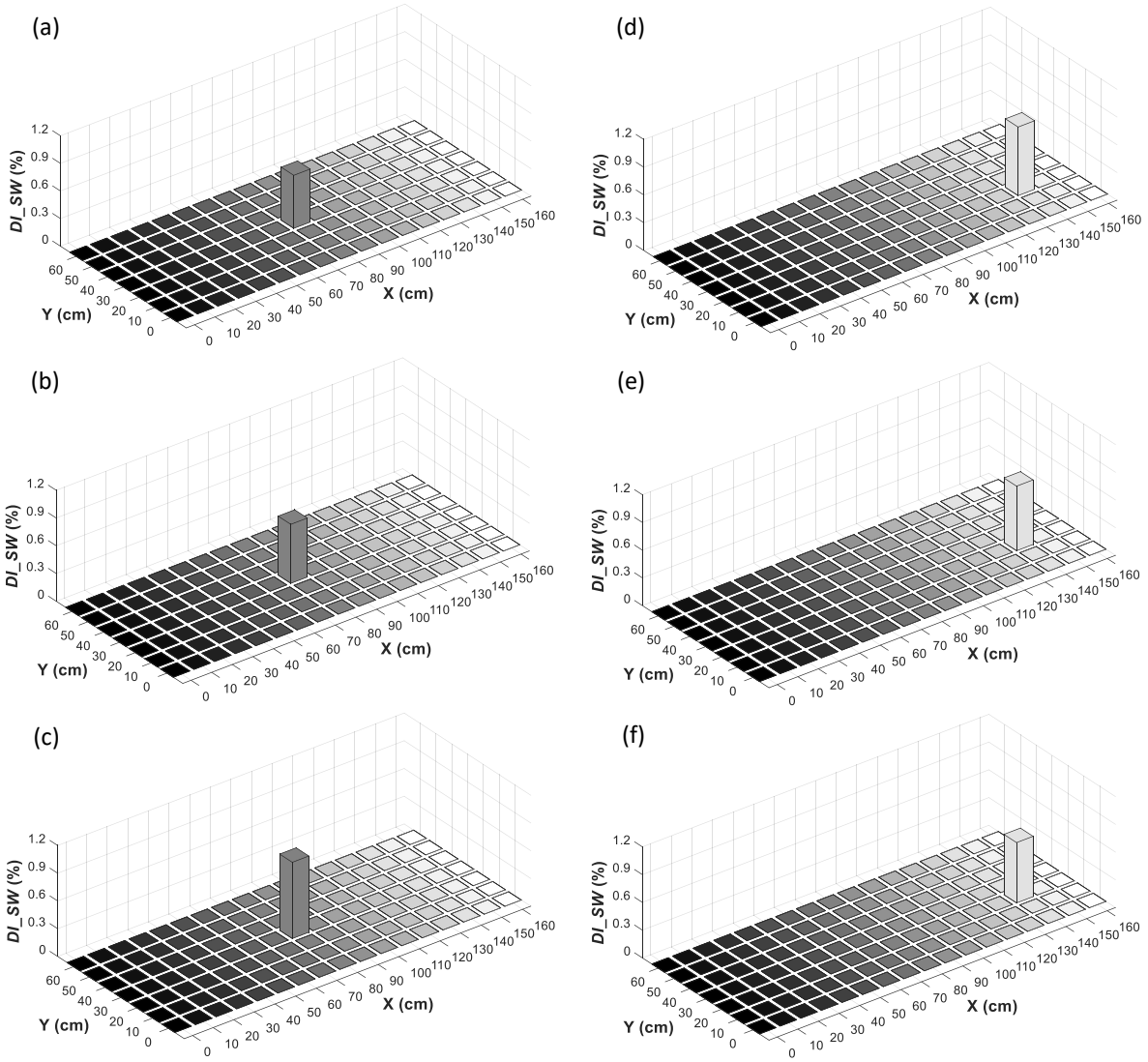

Fig. 17. Results of the proposed damage index *DI_SW* with mother wavelet db2 in the numerical models: a) S_M_TS; b) S_M_LS; c) S_M_IS; d) S_C_TS; e) S_C_LS and f) S_C_IS.

Fig. 17 shows that in accordance with the reported results in Table 4, use of the mother wavelet db2 for the proposed damage index *DI_SW* provided possibility of precise identification of damages in all the numerical models. Hence, generally it could be stated that wavelet db2 is an appropriate mother wavelet in detecting the location of damage scenarios at the middle and corners of the prestressed concrete slabs. The results of the proposed damage index *DI_SW* using the mother wavelet bior2.2 after applying the damage threshold (Tr_α) in all numerical models are presented in Fig. 18.

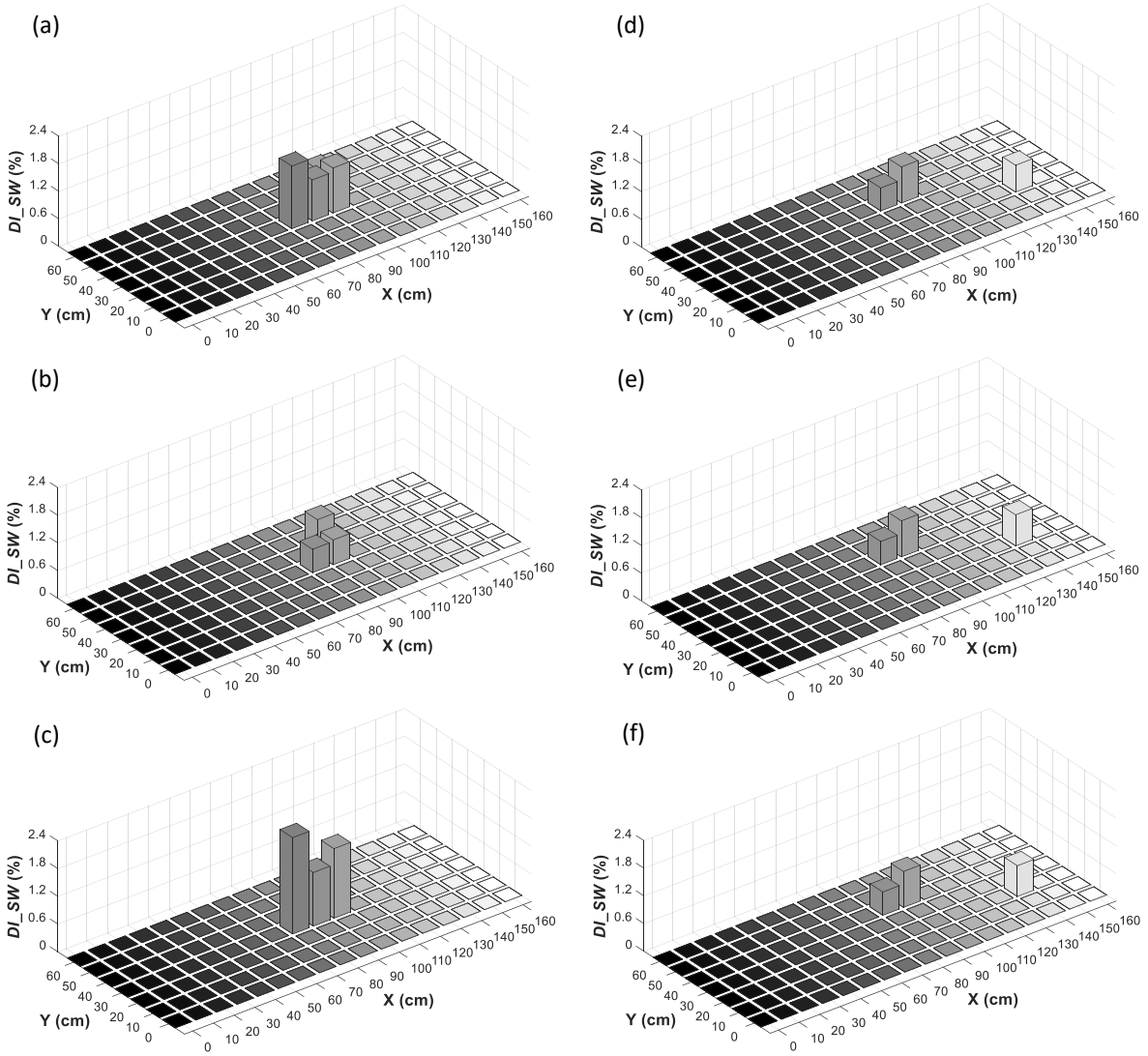

Fig. 18. Results of the proposed damage index *DI_SW* with mother wavelet bior2.2 in the numerical models: a) S_M_TS; b) S_M_LS; c) S_M_IS; d) S_C_TS; e) S_C_LS and f) S_C_IS.

Based on the results presented in Fig. 18 and table 4, the proposed damage index *DI_SW* using the mother wavelet bior2.2, except for S_M_LS numerical model, has been somehow successful in estimating the damage location in the other numerical models. Hence, in comparison to obtained results from using the mother wavelet bior2.2 in the proposed damage index *DI_MW*, is much more efficient. At the end, the results of applying the mother wavelet rbior2.2 in the damage index *DI_SW* after applying the damage threshold (Tr_α) in all numerical models are presented in Fig. 19.

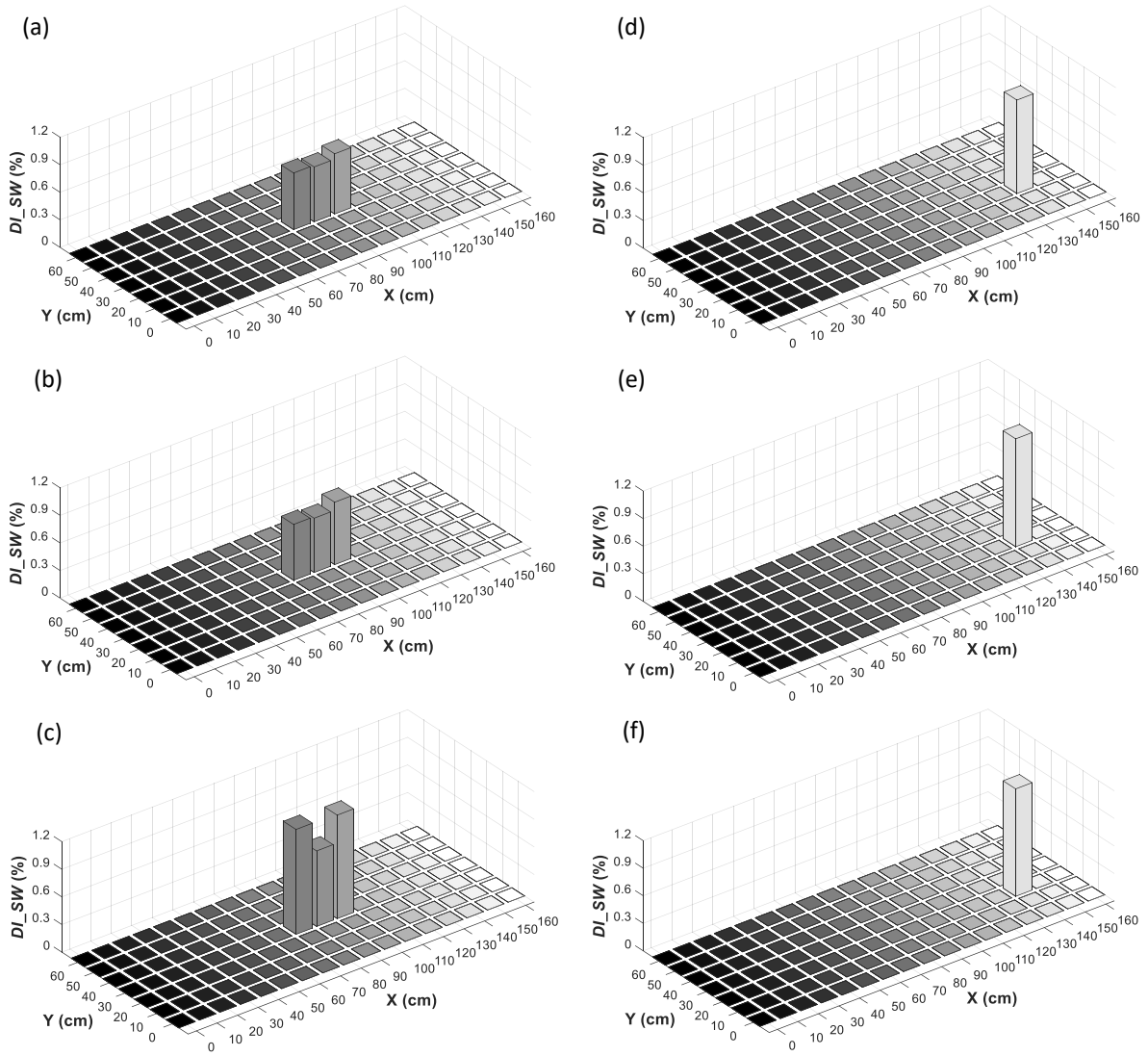

Fig. 19. Results of the proposed damage index *DI_SW* with mother wavelet rbio2.2 in the numerical models: a) S_M_TS; b) S_M_LS; c) S_M_IS; d) S_C_TS; e) S_C_LS and f) S_C_IS.

According to Table 4 and the results presented in Fig. 19, the mother wavelet rbio2.2 in the proposed damage index *DI_SW* has been somehow successful in estimating the damage location in S_M_TS, S_M_LS and S_M_IS numerical models. On the other hand, incorporating this wavelet in the proposed damage index *DI_SW* leads to very desirable results in detecting the damage locations in S_C_TS, S_C_LS and S_C_IS numerical models. Hence, it could be stated that the proposed damage index *DI_SW* using the mother wavelet rbio2.2 has good capability in detecting damages at the corners of the prestressed concrete slabs.

In general, comparing the results obtained from the proposed damage indices: *DI_SA*, *DI_MW* and *DI_SW* in this paper shows that, the best index for detecting damage scenarios in various numerical models is the damage index *DI_SW*. This index is obtained based on the area under the detail coefficients diagram of the wavelet transform applied on the accelerations time histories at each degree of freedom. *DI_SW* damage index, using the mother wavelet db2, is capable of

detecting damages at the middle and corners. In addition, using the mother wavelet rbio2.2, it is capable of detecting damage at the corners of the prestressed concrete slabs. Fig. 20 shows a comparison of using db2 and rbio2.2 as the mother wavelet in proposed damage index *DI_SW* for damage identification in both groups of prestressed concrete slab models, S_M and S_C, with damage scenarios at middle and center of slab, respectively.

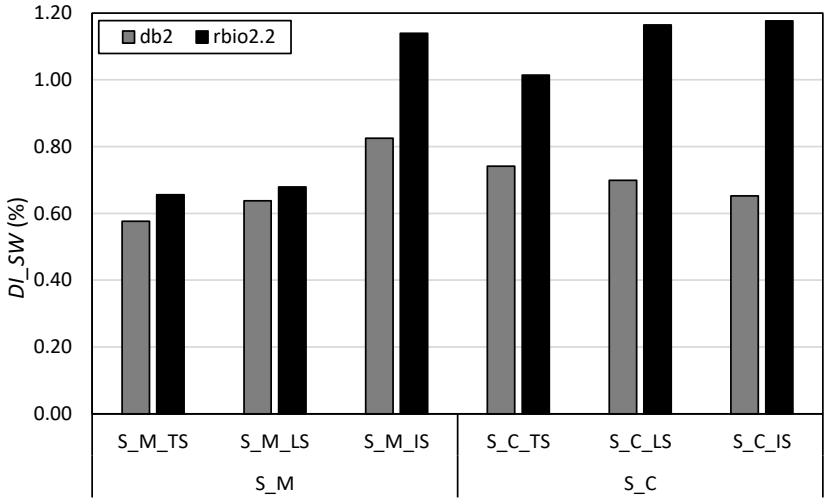

Fig. 20. Comparison the results of using ab2 and rbio2.2 as mother wavelet in the proposed damage index *DI_SW*.

The results of Fig. 20 reveals that in all numerical models of S_M and S_C groups, compared to db2, using rbio2.2 as the mother wavelet causes the damage index *DI_SW* get higher values and hence is more sensitive to all damage scenarios with different types and locations. Moreover, by considering the db2 as the mother wavelet, the proposed damage index *DI_SW*, shows an opposite sensitivity trend to different damage types in the first and second groups of numerical models, S_M and S_C, respectively. In numerical models including damage scenarios at the middle of the prestressed concrete slabs, S_M group, damage index *DI_SW* is more sensitive to inclined, longitudinal and transverse slots (S_M_IS, S_M_LS and S_M_TS models), respectively. On the contrary, transverse, longitudinal and inclined slots, respectively, cause higher values of damage index *DI_SW* in the second group of numerical models, S_C, including damage scenarios at corners of slabs (S_M_TS, S_M_LS and S_M_IS models, respectively). On the other hand, using rbio2.2 as the mother wavelet, causes a permanent trend toward damage type sensitivity and in both groups of numerical models, S_M and S_C, the proposed damage index *DI_SW* is more sensitive to inclined, longitudinal and transverse slots, respectively.

5. Conclusion

In this paper, by focusing on the time histories of vibration responses, it is attempted to detect the location of damage scenarios with different geometric shapes (transverse, longitudinal and inclined slots) and various locations (middle and center) of the prestressed concrete slab models. For this purpose, after being assured of ABAQUS

software capability in modeling an experimental specimen assessed in a previous research, a number of different damage indices were proposed which their inputs were the accelerations time histories corresponding to the degrees of freedom at two states of damaged and undamaged models. These indices were obtained based on the area under diagram of accelerations time histories (denoted by *DI_SA*), maximum detail coefficients (denoted by *DI_MW*) and area under diagram of detail coefficients (denoted by *DI_SW*) in the wavelet transform applied on time histories of acceleration responses. The proposed *DI_MW* and *DI_SW* damage indices use db2, db4, db6 and db8 mother wavelets from Daubechies wavelet family, bior2.2, bior2.4 and bior2.8 from Biorthogonal wavelet family and rbio2.2, rbio2.4 and rbio2.8 from Reverse Biorthogonal family, to detect different damage scenarios. The following conclusions can be drawn from the results of the paper:

- The results show that the proposed damage index *DI_SA*, which was obtained from the area under diagram of accelerations time histories at different degrees of freedom, was not significantly capable in detecting the location of damage scenarios in numerical models of prestressed concrete slabs.
- The damage index *DI_MW*, calculated from difference between the maximum values of the detail coefficients of wavelet transform applied on the accelerations time histories per different degrees of freedom was not capable of detecting damage location in the prestressed concrete slabs using either of Daubechies, Biorthogonal and Reverse Biorthogonal wavelet families.
- Comparison of the proposed damage indices *DI_SA*, *DI_MW* and *DI_SW* shows that the most appropriate index for detecting the damage scenarios in all numerical models is the damage index *DI_SW*. This index is calculated based on the area under the detail coefficients diagram of the wavelet transform applied on the accelerations time histories per each degree of freedom of the prestressed concrete slab models.
- In general, examining the results shows that among all the wavelet families, by applying the mother wavelet db2, the proposed damage index *DI_SW* could detect the damage scenarios at the middle and corners of the prestressed concrete slab models with a well precision. Furthermore, the damage scenarios at the corners of numerical models could be detected properly by using the mother wavelet rbio2.2 in the proposed damage index *DI_SW*.
- The values of the proposed damage index *DI_SW* varies for different damage types and the results show that in all numerical models of prestressed concrete slabs, the *DI_SW* damage index is more sensitive to inclined, longitudinal and transverse slots, respectively.

REFERENCES

[1] Jahangir H, Esfahani MR. Damage localization of Structures Using Adaptive Neuro-Fuzzy Inference System. 7th Natl. Congr. Civ. Eng., Zahedan, Iran: 2013.

[2] Daneshvar MH, Gharighoran A, Zareei SA, Karamodin A. Early damage detection under massive data via innovative hybrid methods: application to a large-scale cable-stayed bridge. Struct Infrastruct Eng 2020:1–19. https://doi.org/10.1080/15732479.2020.1777572.

[3] Jahangir H, Khatibinia M, Kavousi M. Application of Contourlet Transform in Damage Localization and Severity Assessment of Prestressed Concrete Slabs. Soft Comput Civ Eng 2021;5:39–67. https://doi.org/10.22115/SCCE.2021.282138.1301.

[4] Jahangir H, Karamodin A. Structural Behavior Investigation Based on Adaptive Pushover Procedure. 10th Natl. Congr. Civ. Eng., Tehran, Iran: 2015.

[5] Jahangir H, Bagheri M. Evaluation of Seismic Response of Concrete Structures Reinforced by Shape Memory Alloys (Technical Note). Int J Eng 2020;33. https://doi.org/10.5829/ije.2020.33.03c.05.

[6] Jahangir H, Esfahani MR. Numerical Study of Bond – Slip Mechanism in Advanced Externally Bonded Strengthening Composites. KSCE J Civ Eng 2018;22:4509–18. https://doi.org/10.1007/s12205-018-1662-6.

[7] Jahangir H, Esfahani MR. Investigating loading rate and fibre densities influence on SRG - concrete bond behaviour. Steel Compos Struct 2020;34:877–89. https://doi.org/10.12989/scs.2020.34.6.877.

[8] Jahangir H, Esfahani MR. Experimental analysis on tensile strengthening properties of steel and glass fiber reinforced inorganic matrix composites. Sci Iran 2020. https://doi.org/10.24200/SCI.2020.54787.3921.

[9] Bagheri M, Chahkandi A, Jahangir H. Seismic Reliability Analysis of RC Frames Rehabilitated by Glass Fiber-Reinforced Polymers. Int J Civ Eng 2019. https://doi.org/10.1007/s40999-019-00438-x.

[10] Jahangir H, Daneshvar Khoram MH, Esfahani MR. Application of vibration modal data in gradually detecting structural damage (In Persian). 4th Int. Conf. Acoust. Vib., Tehran, Iran: 2014.

[11] Arefzade T, Hosseini Vaez S, Naderpour H, Ezzodin A. Identifying location and severity of multiple cracks in reinforced concrete cantilever beams using modal and wavelet analysis. J Struct Constr Eng 2016;3:72–83.

[12] Altunışık AC, Okur FY, Karaca S, Kahya V. Vibration-based damage detection in beam structures with multiple cracks: modal curvature vs. modal flexibility methods. Nondestruct Test Eval 2019;34:33–53. https://doi.org/10.1080/10589759.2018.1518445.

[13] Daneshvar MH, Gharighoran A, Zareei SA, Karamodin A. Damage Detection of Bridge by Rayleigh-Ritz Method. J Rehabil Civ Eng 2020;8:111–20. https://doi.org/10.22075/JRCE.2019.17603.1337.

[14] Singh J, Roy AK. Wind Pressure Coefficients on Pyramidal Roof of Square Plan Low Rise Double Storey Building. Comput Eng Phys Model 2019;2:1–16. https://doi.org/10.22115/cepm.2019.144599.1043.

[15] Seyedi SR, Keyhani A, Jahangir H. An Energy-Based Damage Detection Algorithm Based on Modal Data. 7th Int. Conf. Seismol. Earthq. Eng., International Institute of Earthquake Engineering and Seismology (IIEES); 2015, p. 335–6.

[16] Pahlevan Mosavari, A. Jahangir H, Esfahani MR. The Effect of Sensor Weight on Obtained Data from Modal Tests (In Persian). 9th Natl. Congr. Civ. Eng., Mashhad, Iran: Ferdowsi University of Mashhad; 2016.

[17] Yang YB, Yang JP. State-of-the-Art Review on Modal Identification and Damage Detection of Bridges by Moving Test Vehicles. Int J Struct Stab Dyn 2018;18:1850025.

https://doi.org/10.1142/S0219455418500256.

[18] Naderpour H, Fakharian P. A synthesis of peak picking method and wavelet packet transform for structural modal identification. KSCE J Civ Eng 2016;20:2859–67. https://doi.org/10.1007/s12205-016-0523-4.

[19] Jahangir H, Esfahani MR. Structural Damage Identification Based on Modal Data and Wavelet Analysis. 3rd Natl. Conf. Earthq. Struct., Kerman, Iran: 2012.

[20] Avci O. Amplitude-Dependent Damping in Vibration Serviceability: Case of a Laboratory Footbridge. J Archit Eng 2016;22:04016005. https://doi.org/10.1061/(ASCE)AE.1943-5568.0000211.

[21] Amabili M. Nonlinear damping in large-amplitude vibrations: modelling and experiments. Nonlinear Dyn 2018;93:5–18. https://doi.org/10.1007/s11071-017-3889-z.

[22] Li W, Vu V-H, Liu Z, Thomas M, Hazel B. Extraction of modal parameters for identification of time-varying systems using data-driven stochastic subspace identification. J Vib Control 2018;24:4781–96. https://doi.org/10.1177/1077546317734670.

[23] Lu L, Song H, Huang C. Effects of random damages on dynamic behavior of metallic sandwich panel with truss core. Compos Part B Eng 2017;116:278–90. https://doi.org/10.1016/j.compositesb.2016.10.051.

[24] Rezazadeh Eidgahee D, Rafiean AH, Haddad A. A Novel Formulation for the Compressive Strength of IBP-Based Geopolymer Stabilized Clayey Soils Using ANN and GMDH-NN Approaches. Iran J Sci Technol Trans Civ Eng 2019. https://doi.org/10.1007/s40996-019-00263-1.

[25] Rezazadeh Eidgahee D, Haddad A, Naderpour H. Evaluation of shear strength parameters of granulated waste rubber using artificial neural networks and group method of data handling. Sci Iran 2019;26:3233–44. https://doi.org/10.24200/sci.2018.5663.1408.

[26] Naderpour H, Rezazadeh Eidgahee D, Fakharian P, Rafiean AH, Kalantari SM. A new proposed approach for moment capacity estimation of ferrocement members using Group Method of Data Handling. Eng Sci Technol an Int J 2020;23:382–91. https://doi.org/10.1016/j.jestch.2019.05.013.

[27] Jahangir H, Rezazadeh Eidgahee D. A new and robust hybrid artificial bee colony algorithm – ANN model for FRP-concrete bond strength evaluation. Compos Struct 2021;257:113160. https://doi.org/10.1016/J.COMPSTRUCT.2020.113160.

[28] Ghorbani B, Arulrajah A, Narsilio G, Horpibulsuk S, Leong M. Resilient moduli of demolition wastes in geothermal pavements: Experimental testing and ANFIS modelling. Transp Geotech 2021;29:100592. https://doi.org/10.1016/j.trgeo.2021.100592.

[29] Ghorbani B, Arulrajah A, Narsilio G, Horpibulsuk S. Experimental investigation and modelling the deformation properties of demolition wastes subjected to freeze–thaw cycles using ANN and SVR. Constr Build Mater 2020;258:119688. https://doi.org/10.1016/j.conbuildmat.2020.119688.

[30] Sadrossadat E, Ghorbani B, Hamooni M, Moradpoor Sheikhkanloo MH. Numerical formulation of confined compressive strength and strain of circular reinforced concrete columns using gene expression programming approach. Struct Concr 2018;19:783–94. https://doi.org/10.1002/suco.201700131.

[31] Kiran KKH, Kori JG. Controlling Blast Loading of the Structural System by Cladding Material. Comput Eng Phys Model 2018;1:79–99. https://doi.org/10.22115/cepm.2018.14129

4.1038.

[32] Law SS, Li XY, Zhu XQ, Chan SL. Structural damage detection from wavelet packet sensitivity. Eng Struct 2005;27:1339–48. https://doi.org/10.1016/j.engstruct.2005.03.014.

[33] Li F, Meng G, Ye L, Lu Y, Kageyama K. Dispersion analysis of Lamb waves and damage detection for aluminum structures using ridge in the time-scale domain. Meas Sci Technol 2009;20:095704. https://doi.org/10.1088/0957-0233/20/9/095704.

[34] Vieira Filho J, Baptista FG, Inman DJ. Time-domain analysis of piezoelectric impedance-based structural health monitoring using multilevel wavelet decomposition. Mech Syst Signal Process 2011;25:1550–8. https://doi.org/10.1016/j.ymssp.2010.12.003.

[35] Rauter N, Lammering R. Impact Damage Detection in Composite Structures Considering Nonlinear Lamb Wave Propagation. Mech Adv Mater Struct 2015;22:44–51. https://doi.org/10.1080/15376494.2014.907950.

[36] Patel SS, Chourasia AP, Panigrahi SK, Parashar J, Parvez N, Kumar M. Damage Identification of RC Structures Using Wavelet Transformation. Procedia Eng 2016;144:336–42. https://doi.org/10.1016/j.proeng.2016.05.141.

[37] Qu H, Li T, Chen G. Adaptive wavelet transform: Definition, parameter optimization algorithms, and application for concrete delamination detection from impact echo responses. Struct Heal Monit 2018:147592171877620. https://doi.org/10.1177/1475921718776200.

[38] Naito H, Bolander JE. Damage detection method for RC members using local vibration testing. Eng Struct 2019;178:361–74. https://doi.org/10.1016/j.engstruct.2018.10.031.

[39] Jahangir H, Esfahani MR. Strain of Newly – Developed Composites Relationship in Flexural Tests (In Persian). J Struct Constr Eng 2018;5:92–107. https://doi.org/10.22065/jsce.2017.91828.1255.

[40] Ghalehnovi M, Yousefi M, Karimipour A, de Brito J, Norooziyan M. Investigation of the Behaviour of Steel-Concrete-Steel Sandwich Slabs with Bi-Directional Corrugated-Strip Connectors. Appl Sci 2020;10:8647. https://doi.org/10.3390/app10238647.

[41] Chaboki HR, Ghalehnovi M, Karimipour A, de Brito J, Khatibinia M. Shear behaviour of concrete beams with recycled aggregate and steel fibres. Constr Build Mater 2019;204:809–27. https://doi.org/10.1016/j.conbuildmat.2019.01.130.

[42] Karimipour A, Edalati M. Shear and flexural performance of low, normal and high-strength concrete beams reinforced with longitudinal SMA, GFRP and steel rebars. Eng Struct 2020;221:111086. https://doi.org/10.1016/j.engstruct.2020.111086.

[43] Karimipour A, Ghalehnovi M. Comparison of the effect of the steel and polypropylene fibres on the flexural behaviour of recycled aggregate concrete beams. Structures 2021;29:129–46. https://doi.org/10.1016/j.istruc.2020.11.013.

[44] Ghalehnovi M, Karimipour A, Anvari A, de Brito J. Flexural strength enhancement of recycled aggregate concrete beams with steel fibre-reinforced concrete jacket. Eng Struct 2021;240:112325. https://doi.org/10.1016/j.engstruct.2021.112325.

[45] Jahangir H, Bagheri M, Delavari SMJ. Cyclic Behavior Assessment of Steel Bar Hysteretic Dampers Using Multiple Nonlinear Regression Approach. Iran J Sci Technol Trans Civ Eng 2021;45:1227–51. https://doi.org/10.1007/s40996-020-00497-4.

[46] Mallat S. A wavelet tour of signal processing. London, UK: Academic Press;

1999.

[47] Hanteh M, Rezaifar O, Gholhaki M. Selecting the appropriate wavelet function in the damage detection of precast panel building based on experimental results and numerical method. Sharif J Civ Eng 2021. https://doi.org/10.24200/J30.2020.56237.2812.

[48] Hanteh M, Rezaifar O, Gholhaki M. Selecting the appropriate wavelet function in the damage detection of precast full panel building based on experimental results and wavelet analysis. J Civ Struct Heal Monit 2021;11:1013–36. https://doi.org/10.1007/s13349-021-00497-6.

[49] Ovanesova AV, Suárez LE. Applications of wavelet transforms to damage detection in frame structures. Eng Struct 2004;26:39–49. https://doi.org/10.1016/j.engstruct.2003.08.009.

[50] Fakharian P. Structural Damage Detection Using Wavelet Packet Transform and Improved Peak-Picking Method. Semnan University, 2014.

[51] Fakharian P, Naderpour H. Damage Severity Quantification Using Wavelet Packet Transform and Peak Picking Method. Pract Period Struct Des Constr 2022;27. https://doi.org/10.1061/(ASCE)SC.1943-5576.0000639.

[52] Hanteh M, Rezaifar O, Gholhaki M. Damage Detection in Precast Full Panel Building Based on Experimental Results and Continuous Wavelet Analysis Analytical Method. Modares Civ Eng J 2021;21.

[53] Rasouli A, Kourehli SS, Ghodrati Amiri G, Kheyroddin A. A Two-Stage Method for Structural Damage Prognosis in Shear Frames Based on Story Displacement Index and Modal Residual Force. Adv Civ Eng 2015;2015:1–15. https://doi.org/10.1155/2015/527537.

[54] Gao RX, Yan R. Wavelets: Theory and applications for manufacturing. Boston, MA: Springer US; 2011. https://doi.org/10.1007/978-1-4419-1545-0.

[55] Hanteh M, Rezaifar O. Damage detection in precast full panel building by continuous wavelet analysis analytical method. Structures 2021;29:701–13. https://doi.org/10.1016/j.istruc.2020.12.002.

[56] Pahlevan Mosavari M. Damage detection on slabs using modal analysis. Ferdowsi University of Mashhad, 2014.

[57] Lubliner J, Oliver J, Oller S, Oñate E. A plastic-damage model for concrete. Int J Solids Struct 1989;25:299–326. https://doi.org/10.1016/0020-7683(89)90050-4.

[58] Oñate E, Oller S, Oliver J, Lubliner J. A constitutive model for cracking of concrete based on the incremental theory of plasticity. Eng Comput 1988;5:309–19. https://doi.org/10.1108/eb023750.

[59] Oller S, Oñate E, Miquel J, Botello S. A plastic damage constitutive model for composite materials. Int J Solids Struct 1996;33:2501–18. https://doi.org/10.1016/0020-7683(95)00161-1.

[60] Pappalardo CM, Guida D. Adjoint-based optimization procedure for active vibration control of nonlinear mechanical systems. J Dyn Syst Meas Control 2017;139:081010. https://doi.org/10.1115/1.4035609.

[61] Sohn H, Czarnecki JA, Farrar CR. Structural Health Monitoring Using Statistical Process Control. J Struct Eng 2000;126:1356–63. https://doi.org/10.1061/(ASCE)0733-9445(2000)126:11(1356).

[62] Sun Z, Chang CC. Statistical Wavelet-Based Method for Structural Health Monitoring. J Struct Eng 2004;130:1055–62. https://doi.org/10.1061/(ASCE)0733-9445(2004)130:7(1055).

[63] Han J-G, Ren W-X, Sun Z-S. Wavelet packet based damage identification of beam structures. Int J Solids Struct 2005;42:6610–27. https://doi.org/10.1016/j.ijsolstr.2005.04.031.